# Are Anion Radicals Nucleophiles and/or Outersphere Electron Donors? An Ab Initio Study of the Reaction of Ethylene and Formaldehyde Anion Radicals with Methyl Fluoride and Chloride

**Juan Bertran,*,[1a] Iluminada Gallardo,[1a] Miquel Moreno,[1a] and Jean-Michel Savéant*,[1b]**

*Contribution from the Departament de Quimica, Unitat de Quimica Fisica, Universitat Autonoma de Barcelona, 08193, Bellaterra, Barcelona, Spain, and the Laboratoire d'Electrochimie Moléculaire de l'Université Denis Diderot, Unité Associée au CNRS No 438, 2 place Jussieu, 75251 Paris Cedex 05, France*

*Received November 1, 1995. Revised Manuscript Received March 27, 1996*[⊗]

**Abstract:** Ab initio calculations combined with an intrinsic reaction coordinate analysis of the title reactions have allowed the identification as well as the geometric and thermodynamic characterization of two types of reaction paths on the same potential energy hypersurface. One involves an outersphere electron transfer from the anion radical which dissociatively reduces the methyl halide acceptor into the methyl radical and the halide ion. The other pathway leads to substitution (two pathways leading to O- and C-substitution repectively in the case of $CH_2{=}O^{\bullet -}$). The substitution transition states have a tighter geometry than the outersphere transition state and may be viewed equivalently as $S_N2$ reactions or innersphere electron transfers concerted with bond cleavage and bond formation. In the competition between the two types of processes, because of bonded interactions in the transition state, $S_N2$ substitution has a lower energy barrier than the outersphere reaction. Owing to the looser geometry of its transition state, entropy favors the outersphere pathway. This factor is not sufficient to reverse the free energy balance with the reactants investigated but this is predicted to occur with sterically hindered systems.

Because it stands at the crossover of single electron transfer and electron-pair transfer chemistries, the title question has received active attention during the last ten years. In an early study,[2] it was observed that the reaction of optically active 2-octyl halides with anthracene anion radical in *N*,*N*′-dimethylformamide (DMF) yields detectable amounts of inversion products (5, 8, and 11% with the iodide, bromide and chloride, respectively) pointing to a competition between an $S_N2$ type reaction and an outersphere electron transfer pathway (ET) producing the alkyl radical which then couples with a second molecule of anthracene anion radical. It is noteworthy that the reaction of the more reducing quinoxaline anion radical with optically active 2-octyl bromide in DMF results in complete racemization.[3] Further evidence for the occurrence of the outersphere electron transfer pathway in the reaction of aromatic anion radicals with alkyl halides was provided by the fact that the follow-up coupling of the radical with the anion radical competes with the electron transfer reduction of the former by the latter thus regenerating the molecule from which the anion radical derives. Thus, when the anion radical is produced electrochemically, the current is endowed with a partial catalytic character resulting from the regeneration of the anion radical parent.[4−6] This indirect electrochemical approach has allowed one to comparatively show that steric hindrance in the acceptor favors the outersphere electron transfer route.[3,7] The same trend has been demonstrated by application of the dissociative electron transfer theory[6,8] to the reaction.[8d] It is also worth noting that in the reaction of anthracene anion radical with a series of methyl derivatives in DMF the contribution of the outersphere electron transfer pathway increases in the following order: $CH_3Cl > CH_3Br > CH_3I > CH_3S(CH_3)_2^+$.[9]

Another important feature of the ET/$S_N2$ dichotomy concerns the entropy of activation. It has been shown that the entropy of activation of the reaction of aromatic anion radicals with alkyl halides augments as the contribution of the ET pathway increases under the influence of more steric hindrance.[7,10] This observation indicates that spatial order in the ET transition state is less than in the $S_N2$ transition state.

Two conceptions of the respective contributions of the ET and $S_N2$ pathways to the reaction of anion radicals have emerged from the above studies. For one of them, the reaction mechanism involves two competitive pathways, implying the existence of two different transition states on the potential energy hypersurface characterizing the reaction.[6−8d] The other conception is that ET and $S_N2$ are the two extremes of a continuous mechanistic spectrum,[5,11,12] implying that a single transition state is to be found on the potential energy hypersurface.[13]

[⊗] Abstract published in *Advance ACS Abstracts,* June 1, 1996.

(1) (a) Universitat Autonoma de Barcelona. (b) Université Denis Diderot.
(2) Herbert, E.; Mazaleyrat, J-P.; Welwart, Z.; Nadjo, L.; Savéant, J.-M. *Nouv. J. Chem.* **1985**, *9*, 75.
(3) Daasberg, K.; Hansen, J. N.; Lund, H. *Acta Chem. Scand.* **1990**, *44*, 711.
(4) (a) Andrieux, C. P.; Gallardo; I.; Savéant, J.-M.; Su, K. B. *J. Am. Chem. Soc.* **1986**, *108*, 638. (b) Nadjo, L.; Savéant, J.-M.; Su, K. B. *J. Electroanal. Chem.* **1985**, *186*, 23.
(5) Lund, T.; Lund, H. *Acta Chem. Scand. Ser. B* **1986**, *40*, 470.
(6) Savéant, J.-M. Single Electron Transfer and Nucleophilic Substitution in *Advances in Physical Organic Chemistry;* Bethel, D., Ed., Academic Press: New York, 1990; Vol. 26, pp 1−30.
(7) Lexa, D.; Savéant, J.-M.; Su, K. B.; Wang, D. L. *J. Am. Chem. Soc.* **1988**, *110*, 7617.
(8) (a) Savéant, J.-M. *J. Am. Chem. Soc.* **1987**, *109*, 6788. (b) Savéant, J.-M. *Acc. Chem. Res.* **1993**, *26*, 455. (c) Savéant, J.-M. Dissociative Electron Transfer in *Advances in Electron Transfer Chemistry;* Mariano, P. S., Ed.; JAI Press: New York, 1994; Vol. 4, pp 53−116. (d) Savéant, J.-M. *J. Am. Chem. Soc.*, **1992**, *114*, 10595.
(9) Daasberg, K.; Christensen, T. B. *Acta Chem. Scand.* **1995**, *49*, 128.
(10) (a) Daasberg, K.; Petersen, S. U.; Lund, H. *Acta Chem. Scand.* **1991**, *45*, 470. (b) Andrieux, C. P.; Delgado, G.; Savéant, J.-M.; Su, K. B. *J. Electroanal. Chem.* **1993**, *448*, 141.

S0002-7863(95)03679-1 CCC: $12.00 

In the work reported below, we have addressed this question by means of an ab initio quantum chemical investigation of the potential energy hypersurfaces for the following three model reactions: $CH_2{=}CH_2^{\bullet -} + CH_3F$, $CH_2{=}O^{\bullet -} + CH_3F$, $CH_2{=}O^{\bullet -} + CH_3Cl$.[14] The central point we wish to discuss is the existence of two different types of transition states on the same potential energy hypersurface. The respective location and energies of the transition states may be changed by the presence of a polar solvent. However, as discussed later on, qualitative conclusions concerning the competition between the two types of pathways are likely to remain unchanged.

## Results and Discussion

**Methodology.** All calculations[15] were carried out with the Gaussian-90[16] and Gaussian-92[17] programs. The double-ζ quality 4-31G basis set was used.[18] A set of d-polarization functions was added to the heavy atoms (exponents: C: 0.50, F: 0.80, Cl: 0.50, O: 0.80) as well as p-polarization functions on hydrogens (exponent: 1.10). Since the investigated systems are anionic, semidiffuse p-functions on heavy atoms (exponents: C: 0.0438, F: 0.055, Cl: 0.049, O: 0.047) were also introduced.

The unrestricted Hartree−Fock method (UHF)[19] was used for all open-shell systems with the exception of a comparative calculation performed with the restricted open-shell Hartree−Fock method (ROHF)[20] in the case of $CH_2{=}O^{\bullet -} + CH_3Cl$. Closed-shell reactants and products were treated by the restricted Hartree−Fock method (RHF).[21] The spin contamination of the UHF results was found to be small, all $\langle S^2 \rangle$ values ranging between 0.75 and 0.78. Correlation energy was introduced according to the Möller−Plesset perturbation treatment up to second order (MP2).[22] Inner shells were excluded from the correlation energy calculations (frozen-core approximation).

Geometries of the stationary points were optimized both at the Hartree−Fock level (RHF or UHF) and the MP2 level by means of the Schlegel gradient algorithm.[23] The nature of the stationary points was deduced from the analytical second derivatives of the energies:[24] no imaginary frequencies for minima, one imaginary frequency for saddle points (transition states). The second derivatives were also used to obtain the various thermodynamic parameters, including the zero-point energy and the entropy from the usual relationships within the ideal gas, rigid rotor, and harmonic oscillator models.[25]

The nature of the reactant and products systems linked to the transition states was assigned by the Intrinsic Reaction Coordinate (IRC) method at the HF level. The IRC is dynamically defined as a minimum energy trajectory that goes infinitely slowly from the transition state to either reactants or products. Its initial direction at the transition state is given by the normal mode of imaginary frequency (the transition vector).[26a] When mass-weighted Cartesian coordinates are used, the IRC provides the steepest descent path or minimum energy path.[26a,b] For other systems of coordinates, the IRC can also be obtained by following the instantaneous acceleration vector in mass-weighted internal coordinates and transforming the resulting path into mass-weighted Cartesian coordinates by means of the Wilson G matrix.[26c] In this work, the IRC has been determined in mass-weighted internal coordinates with a step size of 0.05 in atomic units using an algorithm described in ref 26c.

The charges and spin densities on the main atoms were obtained by a Mulliken population analysis.

The main characteristics of the minima and transition states in terms of energies, entropy, free energy and Mulliken charge distribution are summarized in Table 1. The distributions of charges (with hydrogen charges added to the heavy atom to which they are bonded) are shown in a more detailed manner in Chart 1.

### $CH_2{=}CH_2^{\bullet -} + CH_3$

A minimum energy structure, where the two reactants are only slightly bonded, was first located. This reactant cluster structure, RC, is shown in Figure 1. At this point, charge transfer from the alkene anion radical to methyl fluoride is very small (Table 1 and Chart 1).

Starting from this structure, a reaction coordinate calculation was carried out in which one of the methyl fluoride carbon−ethylene carbon distances, viz., the smallest, was progressively shortened while optimizing the other geometrical parameters. From the maximum energy point thus obtained, a first transition state was then located. It was found to have the geometry depicted in Figure 1 ($S_N2$-TS). A charge transfer of 0.30 au from the anion radical to methyl fluoride has already taken place at this stage. The direction of the transition vector (i.e., the direction of negative curvature of the potential) toward products is also shown in Figure 1. It is clearly seen that it points to the formation of the substitution products, propyl radical + fluoride ion. We may therefore assign this transition to an $S_N2$-type substitution reaction.

Characterization of an outersphere electron transfer transition state was a more difficult task. This is not really surprising if one takes into account that such a reaction may not involve drastic geometrical changes in the ethylene reactant. However, due to the fact that $CH_3F$ is dissociative toward electron transfer, it was possible to emulate electron transfer by enlarging the

(11) Lund, T.; Lund, H. *Acta Chem. Scand. Ser. B* **1988**, *42*, 269.
(12) Pross, A. A General Approach to Organic Reactivity: The Configuration Mixing Model. In *Advances in Physical Organic Chemistry;* Bethel, D., Ed.; Academic Press: New York, 1985; Vol. 21, pp 99−196.
(13) (a) Closely related to this conception is the contention that, with very few exceptions, homogeneous electron transfer reactions should be regarded as innersphere rather than outersphere processes with a strong resonance energy and a tight geometry in their transition states.[13b,c] See, however, a discussion of this point in ref 8d. (b) Eberson, L.; Shaik, S. S. *J. Am. Chem. Soc.* **1990**, *112*, 4484. (c) Cho, J. K.; Shaik, S. S. *J. Am. Chem. Soc.* **1991**, *113*, 9890.
(14) (a) During the completion of this work, another ab initio quantum chemical study of the latter reaction[14b] has appeared describing results that are substantially different from ours as will be discussed in the following sections. (b) Sastry, G. N.; Shaik, S. S. *J. Am. Chem. Soc.* **1995**, *117*, 3290.
(15) A complete description of the geometries in GAUSSIAN data format may be found in the supporting information section.
(16) *Gaussian 90;* Frisch, M. J.; Head-Gordon, M.; Trucks, G. W.; Foresman, J. B.; Schlegel, H. B.; Raghavachari, K.; Robb, M. A.; Binkley, J. S.; Gonzalez, C.; Defrees, D. J.; Fox, D. J.; Whiteside, R. A.; Seeger, R.; Melius, C. F.; Baker, J.; Martin, R. L.; Kahn, L. R.; Stewart, J. J. P.; Topiol, S.; Pople, J. A. Gaussian, Inc.: Pittsburgh, PA, 1990.
(17) *Gaussian 92;* Frisch, M. J.; Trucks, G. W.; Head-Gordon, M.; Gill, P. M. W.; Wong, M. W.; Foresman, J. B.; Johnson, B. J.; Schlegel, H. B.; Robb, M. A.; Reploge, E. S.; Gomperts, R.; Andrés, J. L.; Raghavachari, K.; Binkley, J. S.; Gonzalez, C.; Martin, R. L.; Fox, D. J.; Defrees, D. J.; Baker, J.; Stewart, J. J. P.; Pople, J. A. Gaussian, Inc.: Pittsburgh, PA, 1992.
(18) Clark, W. W.; De Lucia, F. C. *J. Mol. Struct.* **1976**, *32*, 29.
(19) Pople, J. A.; Nesbet, R. K. *J. Chem. Phys.* **1974**, *22*, 571.
(20) Binkley, J. S.; Pople, J. A.; Dobosh, P. A. *Mol. Phys.* **1974**, *28*, 1423.
(21) Roothaan, C. C. J. *Rev. Mod. Phys.* **1951**, *23*, 69.
(22) (a) Möller, C.; Plesset, M. S. *Phys. Rev.* **1934**, *46*, 618. (b) Pople, J. A.; Binkley, J. S.; Seeger, R. *Int. J. Quantum Chem. Symp.* **1976**, *10*, 1.
(23) Schlegel, H. B. *J. Comput. Chem.* **1982**, *3*, 214.
(24) (a) Pople, J. A.; Krishnan, R. A.; Schlegel, H. B.; Binkley, J. S. *Int. J. Quantum Chem. Symp.* **1979**, *13*, 225. (b) Head-Gordon, M.; Pople, J. A. *J. Chem. Phys.* **1994**, *220*, 122.
(25) McQuarrie, D. A. *Statistical Mechanics;*. Harper and Row: New York, 1976.
(26) (a) Truhlar, D. G.; Kuppermann, A. *J. Am. Chem. Soc.* **1971**, *93*, 1840. (b) Fukui, K. *Acc. Chem. Res.* **1981**, *14*, 363. (c) Gonzalez, C.; Schlegel, H. B. *J. Phys. Chem.* **1990**, *94*, 5523.

**Table 1.** Energy and Main Charge Transfer Characteristics of the Minima and Transition States[a]

| states | electronic energy | thermal energy + zero point energy | entropic term (−TS) | Gibbs free energy[l] | charge transfer (au) |
|---|---|---|---|---|---|
| reactants | 0.00 (0.00) | 0.00 (0.00) | 0.00 (0.00) | 0.00 (0.00) | 0.00 (0.00) |
| | | $CH_2{=}CH_2^{\bullet-} + CH_3F$ | | | |
| RC[b] | −10.15 (−7.54) | 2.43 (1.76) | 5.92 (5.34) | −2.39 (−1.03) | 0.05 (0.01) |
| C-$S_N$2-TS[c] | 1.87 (15.22) | 1.46 (0.44) | 8.97 (8.99) | 11.71 (24.06) | 0.30 (0.32) |
| ET-TS[d] | 6.12 (13.95) | 2.50 (1.16) | 4.91 (4.68) | 12.94 (19.20) | 0.61 (0.77) |
| C-$S_N$2-PC[e] | −45.48 (−40.80) | 3.45 (2.54) | 7.61 (6.98) | −35.02 (−31.87) | 0.96 (0.99) |
| C-$S_N$2-P[f] | −37.86 (−36.30) | 2.79 (1.81) | 1.41 (1.70) | −33.66 (−32.79) | 1.00 (1.00) |
| ET-PC[g] | −14.96 (−14.87) | 1.59 (−1.26) | 0.18 (−1.11) | −13.78 (−17.83) | 0.99 (0.99) |
| ET-P[h] | −10.55 (−14.17) | −1.71 (−2.55) | −7.97 (2.56) | −19.61 (−23.95) | 1.00 (1.00) |
| | | $CH_2{=}O^{\bullet-} + CH_3F$ | | | |
| RC[b] | −12.71 (−11.59) | 1.09 (1.82) | 4.71 (6.76) | −7.50 (−3.60) | 0.01 (0.01) |
| O-$S_N$-TS[i] | 5.90 (14.73) | 1.02 (1.85) | 9.67 (9.06) | 16.00 (25.05) | 0.24 (0.23) |
| C-$S_N$2-TS[c] | 5.11 (17.73) | 0.93 (1.77) | 9.86 (9.37) | 15.31 (28.28) | 0.36 (0.37) |
| ET-TS[j] | 17.75 (24.61) | 1.13 (1.93) | 5.51 (5.74) | 23.80 (31.69) | 0.97 (1.00) |
| O-$S_N$2-PC[e] | −11.36 (−8.94) | 2.62 (3.45) | 8.02 (7.49) | −1.31 (1.41) | 0.98 (0.98) |
| O-$S_N$2-P[k] | 6.10 (5.32) | 0.71 (1.54) | 2.62 (2.32) | 9.43 (9.18) | 1.00 (1.00) |
| C-$S_N$2-PC[e] | −16.63 (−18.70) | 0.99 (3.59) | 9.24 (7.59) | −6.99 (−8.11) | 0.94 (0.99) |
| C-$S_N$2-P[f] | −1.12 (−12.20) | 2.58 (2.06) | 3.06 (1.81) | 4.52 (−8.33) | 1.00 (1.00) |
| ET-P[h] | 10. 22 (7.68) | −3.30 (−2.78) | −7.97 (−8.41) | −0.46 (−2.92) | 1.00 (1.00) |
| | | $CH_2{=}O^{\bullet-} + CH_3Cl$ | | | |
| RC[b] | −13.07 (−13.13) | 1.15 (1.83) | 4.45 (6.54) | −8.06 (−5.36) | 0.01 (0.02) |
| O-$S_N$-TS[i] | −4.83 (−7.56) | 1.20 (1.93) | 9.14 (8.02) | 4.92 (1.79) | 0.17 (0.14) |
| C-$S_N$2-TS[c] | −5.60 (−4.38) | 0.86 (1.81) | 8.08 (6.73) | 2.75 (3.56) | 0.15 (0.21) |
| ET-TS[j] | 2.43 (5.01) | 1.45 (2.21) | 7.33 (5.07) | 10.62 (11.69) | 0.22 (0.56) |
| O-$S_N$2-PC[e] | −39.75 (−56.00) | 3.52 (4.72) | 7.69 (6.63) | −29.13 (−45.24) | 0.97 (0.99) |
| O-$S_N$2-P[k] | −25.75 (−45.91) | 1.53 (2.58) | 2.84 (2.58) | −21.38 (−40.75) | 1.00 (1.00) |
| C-$S_N$2-PC[e] | −43.87 (−69.16) | 2.48 (6.63) | 8.02 (8.43) | −33.96 (−54.10) | 0.95 (0.97) |
| C-$S_N$2-P[f] | −32.97 (−63.42) | 3.40 (3.10) | 3.28 (2.06) | −26.29 (−58.26) | 1.00 (1.00) |
| ET-P[h] | −21.63 (−43.55) | −2.48 (−1.74) | −7.75 (−8.15) | −31.27 (−52.84) | 1.00 (1.00) |

[a] MP2 optimized geometry and, between parentheses, HF optimized geometry. Energies in kcal/mol. $T = 298$ K. [b] Reactant cluster. [c] C-substitution $S_N2$ transition state. [d] Outersphere electron transfer transition state. [e] C-substitution $S_N2$ product cluster. [f] C-substitution-$S_N2$ separated products. [g] Outersphere electron transfer product cluster. [h] Outersphere electron transfer separated products. [i] O-substitution $S_N2$ transition state. [j] O-substitution $S_N2$ product cluster. [k] O-substitution-$S_N2$ separated products. [l] Obtained by summing the three preceding columns and adding $nRT$ ($n = 1$ for clusters and transition states, $n = 2$ for separated reactants and for $S_N2$ products, $n = 3$ for outersphere electron transfer separated products).

**Chart 1.** Charges in the Transition States for MP2 Geometries

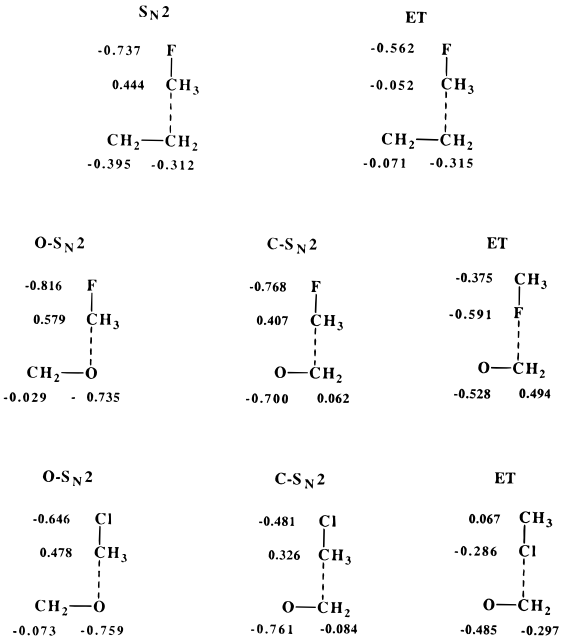


C−F distance while optimizing the other geometrical parameters. Following this approach, care was taken to avoid the triggering of the $S_N2$ reaction during which the C−F distance also enlarges. The structure represented in Figure 1 (ET-TS) was thus identified as a transition state. The direction of the transition vector shown in the Figure confirms that this transition state leads to the dissociative electron transfer products, ethylene + methyl radical + fluoride ion. Mulliken population analysis (Table 1, Chart 1) revealed that 61% of the charge has already been transferred to $CH_3F$ in the transition state.

The geometries of the two transition states are very different, particularly regarding the C−C distance between the two reactants which is much larger in the ET transition state than in the $S_N2$ transition state. It is also worth noting that, in spite of a slightly shorter C−F distance, much more charge has been transferred between the two reactants in the ET transition state than in the $S_N2$ transition state (61% against 30%).

IRC calculations showed that both the $S_N2$ and ET transition states connect with the reactant cluster. It was also found that the $S_N2$ and ET transition states connect with the $S_N2$ and ET product clusters ($S_N2$-PC and ET-PC), respectively, as depicted in Chart 2. The electronic energy of the ET product cluster is only 4.4 kcal/mol below the separated ET products. Since the entropic term favors the separated products by more than 8 kcal/mol, the ET product cluster is not a minimum in terms of free energy and therefore does not appear in Chart 2.

As to the reaction energetics (Table 1), the $S_N2$ path is only slightly more favorable than the ET path, by ca. 5 kcal/mol, in terms of electronic energy. This advantage almost disappears at the level of free energies (Table 1, Chart 2) since, owing to the much more tightly bonded structure of the $S_N2$ transition state (compare Figure 1b,c), the entropy term substantially favors the ET pathway (by ca. 4 kcal/mol) as expected on intuitive grounds.[6−8]

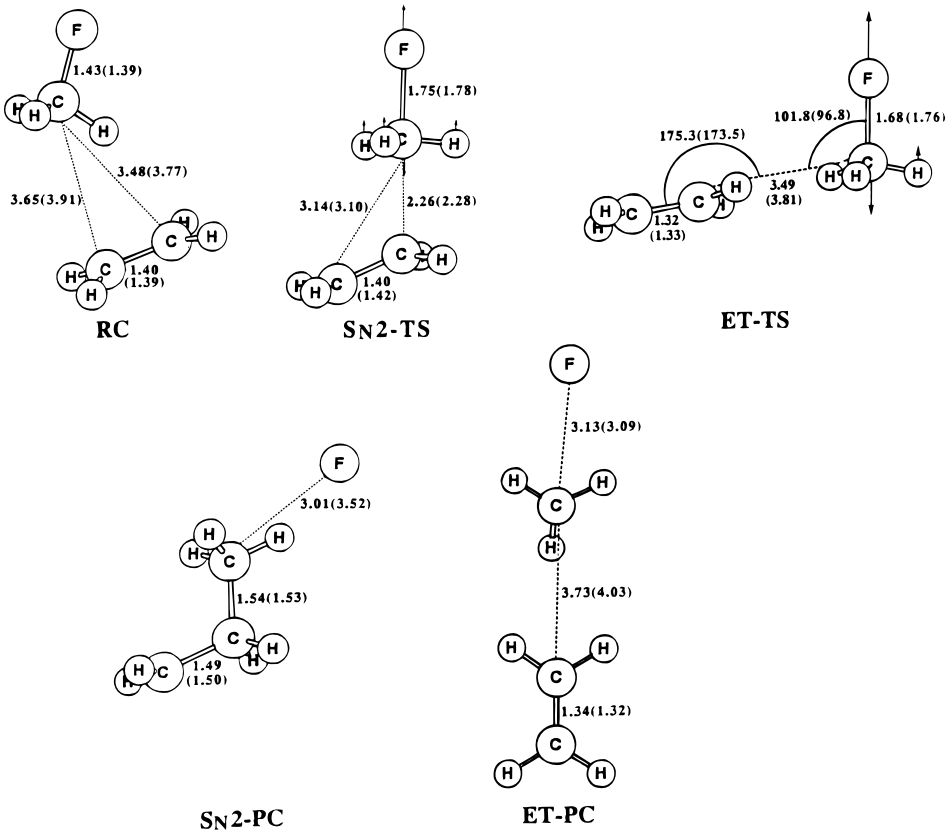


**Figure 1.** $CH_2{=}CH_2^{\bullet -} + CH_3F$. Geometry of the minima and transition states. Distances are in Å and angles in deg. The numbers correspond to the MP2 level and the numbers between parentheses to the HF level.

### $CH_2{=}O^{\bullet -} + CH_3$

The reactant cluster structure (RC in Figure 2) has now an almost colinear structure as a result of the electrostatic interaction between the negatively charged oxygen of the formaldehyde anion radical and the positively charged carbon of $CH_3F$.

Three transition states were located. The direction of the transition vector in each case indicates that they correspond to an O-substitution reaction, a C-substitution reaction, and an outersphere electron transfer reaction yielding $^{\bullet}CH_2OCH_3 + F^-$, $CH_3CH_2O^{\bullet} + F^-$, and $CH_3^{\bullet} + CH_2O + F^-$, respectively. Their geometries are as depicted in Figure 2 (O-$S_N$2-TS, C-$S_N$2-TS, ET-TS, respectively). As expected, in the O-substitution transition state, the formaldehyde oxygen and the carbon and fluorine of $CH_3F$ are almost aligned. In the C-substitution transition state, the formaldehyde carbon and the carbon and fluorine of $CH_3F$ are also close to alignment. The geometry of the outersphere electron transfer transition state is dramatically different. Not only the closest distance between the two reactants is much larger but also the formaldehyde oxygen and carbon are closer from the $CH_3F$ fluorine than from its carbon unlike in the structure of the two other transition states. In spite of a shorter C−F distance, much more charge has been transferred between the two reactants in the ET transition state than in the two $S_N2$ transition states (96% against 24% and 36%).

IRC calculations showed, as depicted in Chart 2, that each of the two substitution transition states connects with the corresponding product cluster, whereas the electron transfer transition state connects with the separated electron transfer products. As to the connection between transition states and reactants, it was found that the two $S_N2$ transition states are linked to the reactant cluster represented in Figure 2, whereas the ET transition states is linked to the separated reactants.

**Chart 2.** Reaction Profiles (Free Energies, MP2 Geometries)

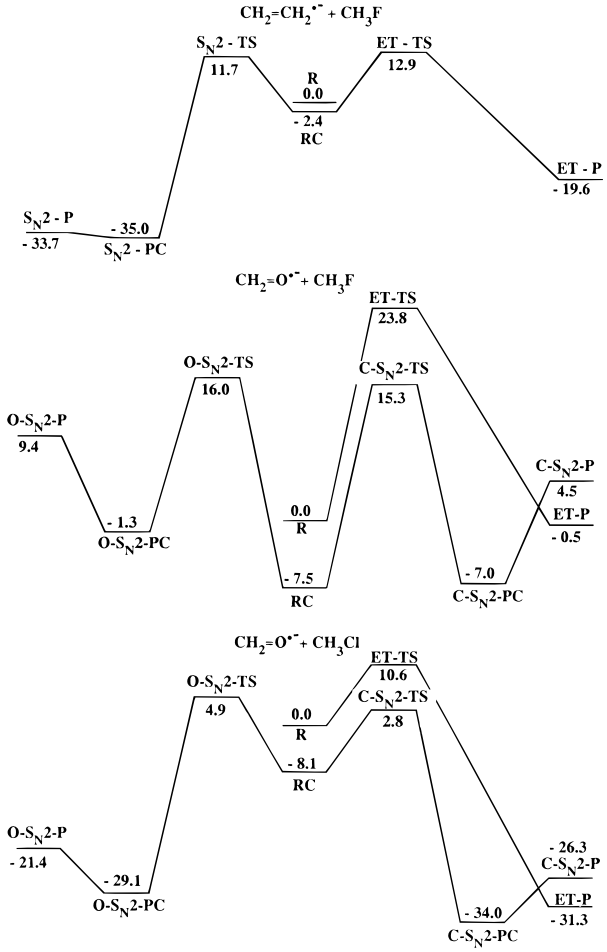

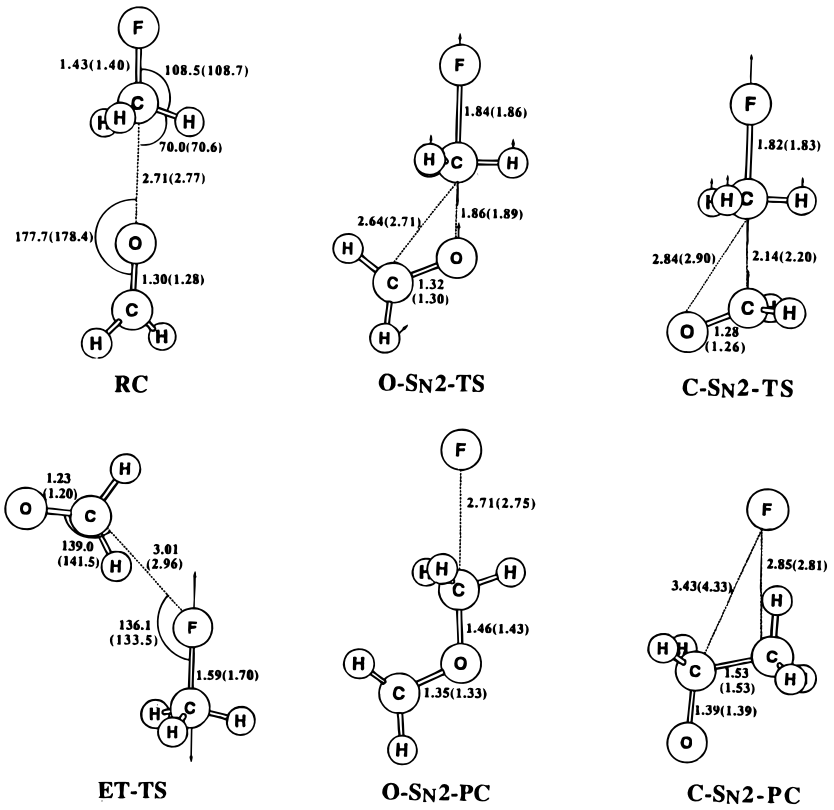


**Figure 2.** $CH_2{=}O^{\bullet-} + CH_3F$. Geometry of the minima and transition states. Distances are in Å and angles in deg. The numbers correspond to the MP2 level and the numbers between parentheses to the HF level.

As seen in Table 1 and Chart 2, C-$S_N2$-substitution is a little favored as compared to O-$S_N2$-substitution, and both reactions are more favorable than the outersphere electron transfer process. Entropy plays again in favor of the outersphere reaction but, since the energy difference is large, this factor does not modify substantially the free energy balance.

### $CH_2{=}O^{\bullet-} + CH_3Cl$

The results (Figure 3,Table 1, Charts 1 and 2) are qualitatively similar to those obtained in the preceding case. The C−O−C−Cl aligned reactant cluster has a somewhat shorter O (anion radical)−C (methyl halide) distance and lower energy resulting from the higher polarizability of the C−Cl bond.

Two transition states were also located and found to be connected with the O-$S_N2$-substitution and the C-$S_N2$-substitution product clusters, respectively. A third transition state, connected with the electron transfer separated products, was also located. This outersphere ET transition state has again a dramatically different geometry, with the chlorine atom pointing toward the carbon of the anion radical moiety, whereas in the O- and C-$S_N2$-substitution transition states, the anion radical oxygen and carbon point toward the $CH_3Cl$ carbon.[27] Here again, in spite of a shorter C−Cl distance, more charge has been transferred between the two reactants in the ET transition state than in the two $S_N2$ transition states (22% against 17% and 15%). The finding that less charge has been transferred in the ET-TS than in the preceding case may be related to the fact that the reaction is more exergonic (by 32 kcal/mol).

Regarding what we have designated by O- and C-$S_N2$-substitutions, the results described in ref 14b are close to ours both in terms of geometries and energies. There is however a big difference between the two sets of results, namely that the outersphere electron transfer transition state was apparently missed in the calculations reported ref 14b. This presumably the reason that what we have called C-$S_N2$-substitution is viewed in ref 14b as an electron transfer process, while the $S_N2$ designation is restricted to O-substitution. A second difference is that we found that the C-$S_N2$-substitution transition state is connected to the C-$S_N2$-substitution product cluster and not to the ET product cluster as reported in ref 14b.

### Outersphere Electron Transfer,[28] Innersphere Electron Transfer,[28] and $S_N2$-Substitution

In all three reactions, the identification of the outersphere electron transfer[28] pathway through the geometrical characteristics of the transition state and its connection with the electron transfer product is straightforward. In each case, the transition state involves, as expected, a shortening of the anion radical C−C or C−O bond en route to the formation of the parent double bonded molecule. For the $CH_2{=}CH_2^{\bullet-} + CH_3F$ reaction, the C−C distance in the anion radical shortens from 1.40 (1.39) Å in the initial reactant cluster to 1.32 (1.33) Å in the TS and to 1.29 (1.32) Å in the neutral final form.[29] For the reaction of formaldehyde anion radical with both methyl fluoride and chloride, the C−O distance shortens from 1.30 (1.28) Å in the initial anionic state to 1.23 (1.20) Å in the TS and to 1.19 (1.18) Å in the final form. In the $CH_2{=}CH_2^{\bullet-} + CH_3F$ substitution, there is no significant variation of the anion radical

(27) At the HF level, some difficulty was encountered in the characterization of the outersphere ET transition state in this case. Through a second derivative analysis of the structure in Figure 3d, a large negative eigenvalue was found whose eigenvector corresponds to an increase of the C−Cl distance in $CH_3Cl$ and a decrease of the formaldehyde anion radical C−O clearly indicating the occurrence of electron transfer. This transition vector is as shown in Figure 3d. However a second, very small, eigenvalue with an imaginary frequency of ca. 20 $cm^{-1}$ was also found. The direction of the corresponding eigenvector indicated a motion of the reactants away one from the other. No such problem was encountered at the MP2 level where only the first imaginary frequency was found.

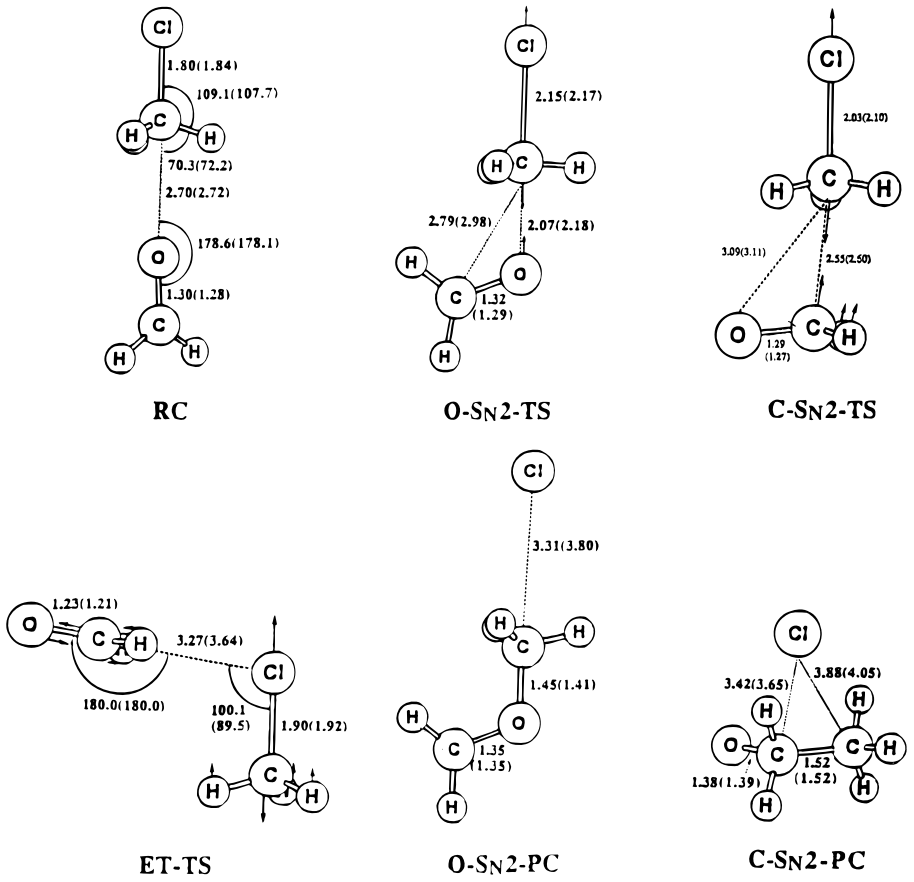


**Figure 3.** $CH_2{=}O^{\bullet -} + CH_3Cl$. Geometry of the minima and transition states. Distances are in Å and angles in deg. The numbers correspond to the MP2 level and the numbers between parentheses to the HF level.

C−C distance in the transition state. With the $CH_2{=}O^{\bullet -} + CH_3F$ and $CH_2{=}O^{\bullet -} + CH_3Cl$ O-substitutions, there is a slight increase of the anion radical C−O bond en route to the formation of the substituted radical product, from 1.30 (1.28) Å in the anion radical to 1.32 (1.30) Å in the TS and to 1.35 (1.40) Å in $CH_3O\text{-}CH_2^{\bullet}$. These observations indicate that, if the reaction is viewed as an innersphere electron transfer,[28] bond breaking and bond formation are progressing at a similar pace along the reaction pathway.

The situation is different with the $CH_2{=}O^{\bullet -} + CH_3F$ C-substitution. A slight shortening of the C−O bond indeed takes place at the TS before the formation of the $CH_3\text{-}CH_2O^{\bullet}$ radical product. The 1.30 (1.28) Å initial C−O distance slightly decreases to 1.28 (1.26) Å in the TS whereas the final C−O distance is enlarged up to 1.39 (1.39) Å. A decrease of the C−O distance is also observed at the TS with methyl chloride albeit to a more modest extent, 1.29 (1.27) Å. IRC HF calculations of both C-substitution reactions showed that, once the transition state has been passed, the shortening of the C−O bond keeps going on down to 1.25 Å with $CH_3F$ and to 1.21 Å with $CH_3Cl$, values that are only slightly larger than the value in formaldehyde, 1.19 Å. This decrease is followed by a sharp increase up to the final value of 1.39 Å.

The structure of the reactant system at the smallest C−O distance deserves a more detailed examination. This structure is represented in Figure 4a together with the charges in the case of $CH_2{=}O^{\bullet -} + CH_3Cl$. Even if charge transfer has substantially progressed at this stage from what it was at the transition state (21%), it is not yet completed (80%, still considering $CH_3Cl$ as a single entity). Consistently, the methyl group has a pronounced radical character (0.71 excess spin density), but it is far from the value, 1, it would have in the methyl radical.

A more detailed picture of this structure is provided by the electronic density in the plane containing approximately the four heavy atoms as represented in Figure 4b. Bond critical points appear between chlorine and the methyl carbon and between this carbon and the formaldehyde carbon. The value of the density at these two bond critical points, 0.025 and 0.040, respectively, is a measure of the bond order.[30] It is thus clear that the C−C that is to be formed upon C-substitution is already present and is stronger than the breaking C−Cl bond.

Thus, this $S_N2$ substitution, which may be viewed as an innersphere electron transfer[28] process, is dissymetric in the sense that, in a first stage, electron transfer and C−Cl elongation progress more than bond formation, while, in a second stage, the addition of the radical-like methyl group on the formaldehyde double bond predominates. There is, however, a substan-

(28) (a) The outersphere/innersphere terminology was originally coined for reactions involving transition metal complexes.[28b,c] In outersphere electron transfers, the coordination spheres remain intact although changes in bond lengths and angles may occur during the reaction. In innersphere processes, bonds are broken and/or formed concertedly with electron transfer. The same terminology may be extended to organic bond-conserving and bond-changing reactions, respectively.[6−8a] Within this framework, a reaction may be of the outersphere type for the donor and of the innersphere type for the acceptor (or vice versa). For simplicity, we use the term outersphere here for reactions that are of the outersphere type for the anion radical donor which transfers dissociatively an electron to the halide acceptor. Innersphere is consequently used for the substitution reactions in which not only a bond is broken but another bond is formed concertedly with electron transfer. (b) Taube, H. Electron Transfer of Complex Ions in Solution, Academic Press: New York, 1970. (c) Espenson, J. H. *Techniques of Chemistry;* Bernasconi, C. F., Ed.; Wiley: New York, 1986; Vol. VI/4E, Part 2, pp 487−563.

(29) The numbers correspond to the MP2 level and the numbers in parentheses to the HF level.

(30) Bader, R. F. W.; Tal, Y.; Anderson, S. G.; Nguyen-Dang, T. T. *Isr. J. Chem.* **1980**, *19*, 8.

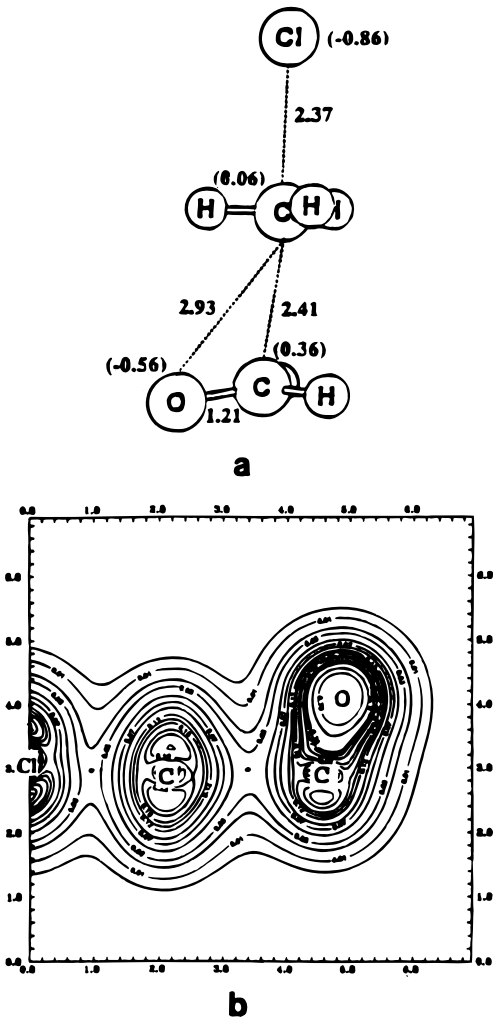


**Figure 4.** $CH_2{=}O^{\bullet-} + CH_3Cl$. State of shortest C−O distance along the IRC path between transition state and products. a: HF geometry and charges. b: Isodensity contour plots of the electronic density of the structure shown in a in the plane containing approximately the four heavy atoms. The dots indicate the bond critical points between the fragments. Distances are in Å and charges in atomic units.

tial overlap of the two phases of the reaction. An essential reason for this dissymetry is the fact that the bond-forming process, which is concerted with electron transfer and bond cleavage, is the addition of a radical to a double bond which expected to be less effective than the coupling of two radicals as it is the case with a closed-shell nucleophile. The fact that O-substitution resembles more the reactions with open-shell nucleophiles than C-substitution is related to the larger charge (0.70 vs 0.30 au) and the smaller spin density (0.16 vs 0.84) born by the oxygen atom of $CH_2{=}O^{\bullet-}$.

Concerning the $CH_2{=}O^{\bullet-} + CH_3Cl$ C-substitution, the difference between our results and those in ref 14 calls for the clarification of two points. One concerns the procedures used for determining the IRC and the other regards spin contamination (and spin polarization). As stated in the Methodology section, we used internal mass-weighted coordinates which, after a simple transformation, is equivalent to using mass-weighted Cartesian coordinates. To further assess this point we repeated the IRC calculation using directly mass-weighted Cartesian coordinates (with the GAMESS program[31]). As expected the results were unchanged. Although not stated in the article, we now know[32] that the results in ref 14b were obtained using internal coordinates not mass-weighted. This method does not lead to the IRC (even if the program "Gaussian" used calls it "IRC") but to a reaction path that may depend on the definition of the internal coordinates employed.

Concerning the second point, we have found, in our UHF calculations, that spin contamination is extremely small, in minima and transition states, the $\langle S^2 \rangle$ values ranging from 0.75 to 0.78. Along the IRC from the C-$S_N2$-TS to the C-substitution products, contamination slightly increases, reaching a value of 0.83 for the structure shown in Figure 4. This is still a small contamination, this state being 97.3% pure if the remaining 2.7% are assigned to contamination by the quartet state (if higher states were assumed, the degree of purity would be even higher). To further assess the importance of spin contamination and to address also the question of spin polarization, we have performed additional calculations at the ROHF level.[20] The C-$S_N2$-TS geometry is practically unaltered, while the total energy is somewhat higher (−3.87 kcal/mol to be compared to −4.38 kcal/mol). Along the IRC from TS to products, a structure very similar to the structure represented in Figure 4 appears (the formaldehyde C−O distance and the formaldehyde−methyl C−C distance are 1.20 and 2.32 Å, respectively, to be compared to 1.21 and 2.41 Å). Beyond this point, however, the C−C distance of the bond to be formed in the $S_N2$ reaction enlarges, formaldehyde C−O distance decreases and the system evolves into the ET products even though the IRC is calculated from mass-weighted coordinates. At the point corresponding to the structure of Figure 4, electron transfer is substantial, and thus the second stage of the reaction that would lead to C−C bond formation resembles the addition of the methyl radical on the formaldehyde double bond. It is known from previous work[33] that ROHF calculations largely overestimate the energy barriers for the addition of radicals to multiple bonds, because they neglect the correlation energy which stabilizes the transition state more than the reactants. For the same reason, the double bond that has to be polarized to lead to the formation of the new C−C bond cannot do so because the ROHF level of calculation does not allow for spin polarization. In UHF calculations, mixing with higher spin states introduce some electron correlation hence lowering the barriers for the addition of radicals to multiple bonds. This is the reason why they are to be preferred in the present case even at the price of some spin contamination.

## Conclusions

The three model reactions that we have investigated are very simplified models of the experimental systems evoked in the introduction, owing to the small size of the molecules selected and because the influence of solvation was not taken into account. Some aspects of their dynamic characteristics are therefore related to the particular molecules that have been examined. However several general conclusions emerge from the results. The most important one is that, in reactions of anion radicals with alkyl halides or other dissociative electron acceptors, an outersphere electron transfer path and $S_N2$ substitution paths (which can be viewed as innersphere electron transfers concerted with bond cleavage and bond formation) can coexist on the same potential energy hypersurface. Anion radicals may thus react both as nucleophiles *and* outersphere electron donors. In the competition, entropy favors the outersphere electron transfer path essentially because its transition state has a less

(31) Schmidt, M. W.; Baldridge, K. K.; Boatz, J. A.; Jensen J. H.; Koseki, S.; Gordon, M. S.; Nguyen, K. A.; Windus, T. L.; Elbert, S. T.*Q.C.P.E. Bulletin*, **1990**, *10*, 52.

(32) Shaik, S., personal communication, December 1995.

(33) Houk, K. N.; Paddon-Row, M. N.; Spellmeyer, D. C.; Rondan, S. *J. Org. Chem.* **1986**, *29*, 1001.

tight geometry than the $S_N2$ substitution transition states. In terms of energy, the innersphere pathways appear easier than the outersphere pathway, albeit to a largely variable extent. It is therefore easily conceivable that steric obstacles may reverse the free energy balance in favor of the outersphere pathway as observed experimentally. Strictly speaking, these conclusions are valid only in the gas phase. The presence of a polar solvent may alter the respective locations and energies of the transition states. The general tendency is that the negative charge is dispersed over a more extended molecular framework in the transition state than in the reactant system. The static effect of solvation should thus slow down all reaction pathways. Solvent reorganization is predicted to further decrease the reactivity. The molecular framework over which the charge is dispersed is less extended in the $S_N2$ TS s than in the ET TS but the degree of charge transfer is less. Compensation of the two effects should thus leave unaltered our main conclusion, namely that $S_N2$ type and ET type transition states may coexist on the same potential energy hypersurface.

**Supporting Information Available:** Complete description of the geometries in GAUSSIAN data format (66 pages). Ordering information is given on any current masthead page.

JA953679T